CONF-820345--5

CONF-820345--5

DE82 011966

HIGH BETA RESULTS IN ISX-B WITH INTENSE NEUTRAL BEAM INJECTION

P. H. Edmonds, S. C. Bates, J. D. Bell, C. E. Bush, B. A. Carreras, L. A. Charlton, W. A. Cooper, J. L. Dunlap, H. C. Howe, D. P. Hutchinson, R. C. Isler, E. A. Lazarus, J. F. Lyon, C. H. Ma, J. K. Munro, M. Murakami, L. E. Murray, G. H. Neilson, D. R. Overbey, V. K. Paré, J. R. Reagan, M. J. Saltmarsh, S. D. Scott, D. J. Sigmar, K. A. Stewart, C. E. Thomas, D. M. Thomas, R. M. Wieland, W. R. Wing, and A. J. Wootton

Oak Ridge National Laboratory*
P.O. Box Y, Oak Ridge, Tennessee 37830, U.S.A.

1. Introduction

For the tokamak to attain reactor-like parameters it is necessary to augment the ohmic heating power. Neutral injection is one such method; high energy neutral particles are injected into the plasma, where they are ionized, trapped, and then thermalized by collisions. This technique has been successfully employed on a large number of tokamaks and has been extensively investigated theoretically.[1] The criteria of success are variously defined: the most obvious effect is in raising ion and electron temperatures. The most spectacular results to date are the approximately 7-keV ion temperatures achieved on the PLT[2] and PDX[3] experiments at Princeton. Another criterion involves the maximum plasma pressure, nkT, which can be achieved. Specifically the plasma beta ($\beta = nkT/B_T^2$), must be >5% for a reactor to be economical.[4] The main objective of the present ISX-B program is to investigate the limits and limiting mechanisms of plasma beta; the highest volume averaged beta achieved to date is 2.5%. The theoretical limits to plasma beta are caused by either loss of equilibrium or the appearance of plasma instability. The former occurs when a separatrix invades the plasma, but such phenomena have not been observed on ISX-B. The latter has been the subject of considerable experimental and theoretical study; it may be reducing the energy confinement in the experiment.

In this paper we describe phenomena which have been observed with up to 2.5 MW of neutral injection. In particular, degradation of confinement with increasing beam power is observed and possible reasons for this are discussed. It is important to understand whether the confinement degradation is due to the high values of plasma pressure or to the form of auxiliary heating used, namely neutral beam injection.

2. Description of Experiment

The ISX-B experiment was designed for the study of high beta plasmas and is a medium sized tokamak with a rectangular cross-section

*Research sponsored by the Office of Fusion Energy, U.S. Department of Energy, under contract W-7405-eng-26 with the Union Carbide Corporation.

vacuum vessel. Auxiliary heating is supplied by two beam lines, designed and built at ORNL. A cross-section view of the machine and the major parameters of the device are shown in Fig. 1. A plan view is shown in Fig. 2 with the main diagnostic and auxiliary apparatus labelled. The beam lines are described in Ref. 5; Fig. 3 shows a schematic of a beam line with the associated parameters and power flows.[5] The history of the experiment is now briefly reviewed. The original ISX experiment was a circular, ohmically heated device built in collaboration with the General Atomic Company. The experimental program concentrated on the study of impurity effects and impurity transport.[6] In 1978 the machine was rebuilt with a rectangular cross section and a poloidal field system allowing elliptic, "D", and circular configurations to be produced.[7] Originally 1.5 MW of neutral injection was available; this was increased to 3 MW in 1980. Both beam lines inject in the same direction and essentially tangential to the magnetic field axis. The primary objective was to explore the properties of circular and noncircular cross-section plasmas with high power neutral beam heating (typically $P_{Pb}/P_{OH} > 10$), in particular to study beta limits in tokamak plasmas. The device was originally run with an ungettered stainless steel first wall, but since February of 1981 titanium gettering has been employed to assist in enlarging the operating regime.

In addition to the high beta program the ISX-B experimental program has a number of elements not discussed in this paper, including impurity transport, toroidal field ripple effects, a pump limiter program, ECH experiments, pellet fueling, plasma-materials interactions, and diagnostic development.

3. Experimental Results

The experimental results detailed here concentrate on the effects of high power neutral injection on confinement. In summary, a deterioration of confinement is observed with high injection powers and at high poloidal betas. The primary objective of the program is to identify the cause of this confinement deterioration and, in particular, to ascertain whether it is a consequence of the heating technique or intrinsic to high beta plasmas. An important experimental procedure used in these measurements is the single parameter scan, in which all but one of the controllable parameters are held constant and this last parameter is varied over as large a range as is practical. The major controllable parameters are the toroidal field (B_T), the plasma current (I_p), the line averaged plasma density ($\bar{n}_e$), and the beam power (P_b). It has not proved possible to scan P_b without making excessive changes in other parameters. Before beginning a scan the plasma conditions are carefully established to produce an optimum discharge (starting where operation is most difficult, e.g., low B_T, high I_p) over the entire scan, and the time history of the variables is adjusted for maximum plasma beta at each point. The extent of the operating range of the tokamak can be seen in Fig. 4. This plot includes essentially all the data analyzed to date. The most significant features are (a) the accessibility of low q operation, down to 2.2, and (b) the extremely high values of the parameter $\bar{n}_e R/B_T$ attained for both circular and noncircular plasmas.

The plasma shape and beta results described here are obtained from poloidal magnetic equilibrium measurements, which consist of measurements of the winding and plasma currents, and point measurements of the external poloidal field.[8] This technique determines $\beta_p + \ell_i/2$; the ℓ_i can be estimated for a given q_a, on the basis of experience and MHD equilibrium simulations, and this estimate used to obtain β_p. The nature of this measurement is such that it includes all the components of the pressure including the fast ions and rotational energy. It has been compared with kinetic measurements of plasma pressure and generally agrees within 20% except for cases with β_p greater than about 2. An important result of this analysis is the calculation of a global energy confinement time, τ_E^*.

Figure 5 shows the details of a discharge, selected for high beta and low q and for two beam co-injection. The turn-on times of the neutral beam sources are staggered and the rise times slowed down to assist the position control. Note that both the plasma density ($\bar{n}_e$) and the plasma current (I_p) are ramped up during the discharge; this is necessary to avoid disruptions. The most important feature of this figure is the plot of τ_E^* vs time, in which the decrease in τ_E^* with increased beam power can clearly be seen. (At early times when β_p and the plasma current are low the correction for the plasma inductance is too large, giving an artificially small confinement time.)

An extensive effort aimed at identifying the parametric dependance of the volume averaged beta gives the empirical relationship:

$$\langle\beta\rangle \propto \frac{I_p^{3/2} P_b^{1/3}}{B_T^2(1+\kappa^2)} .$$

Figure 6 shows a plot of this relationship. A simple rearrangement of this empirical expression gives

$$\tau_E^* \propto (I_p^{3/2})/(P_b^{2/3}) .$$

These relationships are the result of an interactive regression analysis of the experimental data, with fits forced to fractional exponents,[9] and of single parameter scans. They are not supported by any theoretical derivations. All the data described in this paper are subsets of the data displayed in this plot. Figure 7 shows the results of the B_T single parameter scan; since β_p is constant and $\tau_E^* \propto \beta_p$ at constant current, this plot shows the insensitivity of the global confinement time to the toroidal field. The $\langle\beta\rangle \propto B_T^{-2}$ dependance can also be seen; the apparent departure from this relationship at low B_T is due to minor changes in the fixed parameters I_p and plasma radius at low B_T.

Figure 8 shows the results of the I_p single parameter scan. For constant B_T, $\tau_E^* \propto \langle\beta\rangle$, and the continuing improvement in τ_E^* with increasing I_p can clearly be seen.

Time independent profile analysis using Thomson electron scattering and poloidal magnetic data has been augmented by the addition of self-consistent models for both the MHD equilibrium and ion power balance. An interior flux surface geometry is obtained from a fixed boundary "moments" solution of the Grad-Shafranov equation. In this model the toroidal current profile is defined so as to yield a q profile which matches the position of the q = 1 surface as deduced from chordal soft x-ray measurements. The ion component of the required pressure profile comes from a detailed treatment of the ion power balance using a neo-classical heat conduction coefficient multiplier to yield a central T_i in agreement with the ion temperature diagnostics.[10] Conclusions from this calculation include the neoclassical heat conduction coefficient and the power balance. Results of this calculation are shown in Fig. 9, which shows the electron confinement time at half radius as a function of electron density for a range of neutral beam injected powers. The plot shows the deterioration in electron energy confinement with increasing beam power rather dramatically. It should also be noted that Alcator scaling ($\tau_e \propto \bar{n}_e a^2$) is no longer applicable to the high power data.

The neutral injection also affects particle transport, as illustrated in Fig. 10, which shows a plot of line averaged electron density vs time for two discharges, one with neutral injection and one without, with constant fueling gas rate. Although the interpretation of this "density clamp" is obscured by possible changes in wall recycling with beam heating, it indicates a significant deterioration in particle confinement.

There are a number of effects associated with neutral beam heating in addition to the simple deposition of power in the plasma: these include an increase in the central neutral density from "halo neutrals," an increase in impurity levels as a consequence of the neutral beams, and the development of plasma rotation with parallel injection. Code calculations[11] show that the effect of the halo neutrals is insignificant, and impurity spectroscopy shows that the impurity density inside the plasma actually decreases with co-injection.[12] On the other hand, plasma rotation associated with neutral injection is observed, but the measurements are very difficult as they are made from Doppler shift measurements of injected impurities which are expelled from the plasma by beam driven impurity flow reversal. Figure 11 shows the plasma rotation speed in a discharge during the beam power turn-on for a number of different conditions. The impurity line intensities are too small to be detected late in the discharge. Plasma rotation can affect the energy confinement in at least three ways: (a) by introducing an additional loss channel through viscosity, (b) by driving instabilities, and (c) by introducing a radial electric field that modifies the radial transport.

4. Discussion of Results

The conclusion to be drawn from the previously described experimental data is that the ISX-B experiment shows a marked decrease in the efficiency of neutral beam heating for power levels significantly above 1.0 MW. The most obvious possibilities are that the power does not reach the plasma, or that either the fast ions are not produced or are lost before transferring their energy to the plasma. Relative comparisons of plasma effects with either or both beams show that the

indicated beam powers are additive, to the maximum power level that this technique can check (~1.5 MW), which shows that the beam neutrals enter the plasma. An analysis of the fast ion spectra also supports the belief that the fast ions are initially trapped in the tokamak and also that the slowing down is consistent with classical predictions; however, this analysis is very dependent on the assumptions made concerning the local neutral particle density, which itself is very uncertain. The power deposition from the Fokker-Planck calculations[13] agrees well with Monte Carlo calculations;[14] these show small (<10%) losses due to fast ion orbits and charge exchange losses, even at low plasma currents.

A possible channel for the heat loss is through the ions. However, a major difficulty with any explanation involving the ion channel to account for the enhanced heat loss is the relatively small amount of power available to the ions; the ion and electron temperatures are roughly equal, so little power is transferred from the electrons. Moreover, at the injection energies used the power transferred from the fast ions to the plasma ions is about one-half that to the electrons. To explain the power loss by convection and charge exchange would require unrealistically high reflux neutral source terms and temperatures at the plasma edge. For ohmic plasmas the neoclassical ion heat conduction coefficient is in the range of 1-2; with the 2.5 MW of neutral beam heating this increases to 2.5-4. This increase can only account for a small fraction of the total increased power flow. Another possible cause of ion heat loss could be through plasma rotation; rotation speeds approaching the ion sound speed and ion thermal velocity have been observed, possibly enough to drive enhanced loss mechanisms. Experiments with co- and counter-injection show dramatic differences in impurity and particle transport, suggesting that plasma rotation effects are a likely cause for the observed confinement deterioration.

The other branch for the observed enhancement of heat loss with high power injection is the electron channel. The radiation loss is only about 20% of the total power and this fraction does not increase significantly with increased beam power (Fig. 5). Electron-ion heat transfer is relatively small, even with an enhanced heat transfer coefficient, due to the small temperature difference. An evaluation of the power balance shows that the dominant term is electron heat conduction loss; a prime candidate for this enhanced electron conductivity is resistive MHD modes, where the saturated magnetic perturbation is large enough to destroy the integrity of the magnetic surface structure and produce rapid energy transfer from the plasma. The more obvious mode is the 1/1 mode with its driven higher n activity. The reason is that the $m = 1$; $n = 1$ mode is unstable for any beta where $q < 1$, which is the case for usual operation of ISX-B. These modes are experimentally observed. Detailed comparisons between theoretically predicted mode structure and experimental observations have been made,[15] and the agreement is excellent even to the fine grain details of the wave forms, as can be seen in Fig. 12. This mode is not the main cause of the observed confinement deterioration. As is shown in Fig. 13, β_p and τ_E^* remains constant as the toroidal field decreases in spite of the growth of the MHD activity associated with the 1/1 mode. However, the theory also predicts that resistive pressure driven modes become destabilized with increasing β_p. These modes nonlinearly saturate and their n spectrum is broad. They can cause a deterioration of confinement and their calculated effect increases with β_p. They are a good candidate to

explain the degradation of confinement in ISX-B.

It should be realized that although the confinement is deteriorating, no beta limit as such has been observed. The present measurements would indicate that operation at lower toroidal field or at higher plasma currents would produce a higher $<\beta>$ than yet achieved.

5. Conclusion

Experiments on the ISX-B device show a deterioration in confinement at high beam power. In particular the electron energy confinement time falls catastrophically with increasing beam power. The maximum volume averaged beta values achieved are <2.5%; this is much less than would be predicted by extrapolating the low power data. Elongation has not been observed to have any significant effect on the maximum attainable beta, perhaps due to the limited range of both internal and external elongation. The electron energy confinement time does not follow Alcator scaling at high injection powers. There are two likely candidates for the loss of confinement. The phenomena may be β_p specific and caused by the gradual onset of resistive MHD pressure driven modes producing deteriorating confinement through fluctuations in the poloidal magnetic field. Alternatively the phenomena may be specific to the method of heating, neutral injection, being caused, for example, by plasma rotation, where the rotation speed approaches the ion thermal velocity. Experiments are in progress to investigate both of these possibilities. A third neutral beam line, opposite in direction to the existing two, will be installed on the experiment to allow balanced momentum injection; in addition, a heavy ion beam probe will be installed to investigate the radial potential distribution. This probe will also be used to study fluctuations. A number of other diagnostics will also be installed to investigate both the plasma rotation and the plasma fluctuations.

References

1. Sheffield, J., Proc. IEEE 69 (1981) 885.
2. Eubank, H., et al., Phys. Rev. Lett. 43 (1979) 270.
3. Bell, M., et al., to be published in Tenth European Conference on Controlled Fusion and Plasma Physics, September 1981, Moscow, Vol. 2.
4. Steiner, D., Proc. IEEE 63 (1975) 1568.
5. Bates, S. C., et al., ORNL/TM-7452.
6. Colchin, R. J., Jernigan, T. C., J. Nucl. Mater. 63 (1976) 83.
7. Saltmarsh, M. J., J. Vac. Sci. Technol. 17 (1980) 260.
8. Swain, D. W., Neilson, G. H., submitted to Nucl. Fusion (1981).
9. Swain, D. W., et al., Nucl. Fusion 21 (1981) 1409.
10. Wieland, R. M., "A Thomson Scattering Based Analysis Method for ISX-B Plasmas using MHD Geometry," to be published.
11. Murakami, M., et al., in Plasma Physics and Controlled Nuclear Fusion Research (Proc. 8th Int. Conf. Brussels, 1980) 1, IAEA, Vienna (1981) 377.
12. Isler, R. C., et al., Phys. Rev. Lett. 47 (1981) 333.
13. Callen, J. D., et al., in Plasma Physics and Controlled Nuclear Fusion Research (Proc. 5th Int. Conf. Tokyo, 1974) 1, IAEA, Vienna (1975) 645.
14. Goldston, R., et al., PPPL-1733 (1981).
15. Dunlap, J. L., et al., Phys. Rev. Lett. 48 (1982) 538.

ISX-B TOKAMAK FED/VU 78-263R8

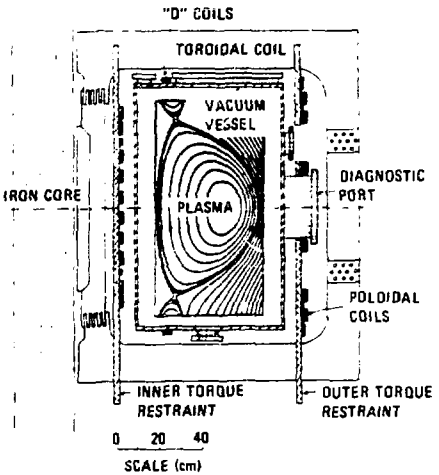

R_0 = .93 m
a = .26 m
$b \leq .42$ m (b/a 1.2-1.6)
B_T .75 → 1.4 T
I_p 60 kA → 220 kA
n_e R/B_T 1 → 10 (x 10^{15} cm^{-2} T^{-1})
LIMITER: TITANIUM CARBIDE COATED CARBON
FIRST WALL: STAINLESS STEEL WITH TITANIUM GETTER
OPERATING PARAMETERS USED IN HIGH BETA STUDIES

Fig. 1. Cross section of ISX-B tokamak with operating parameters.

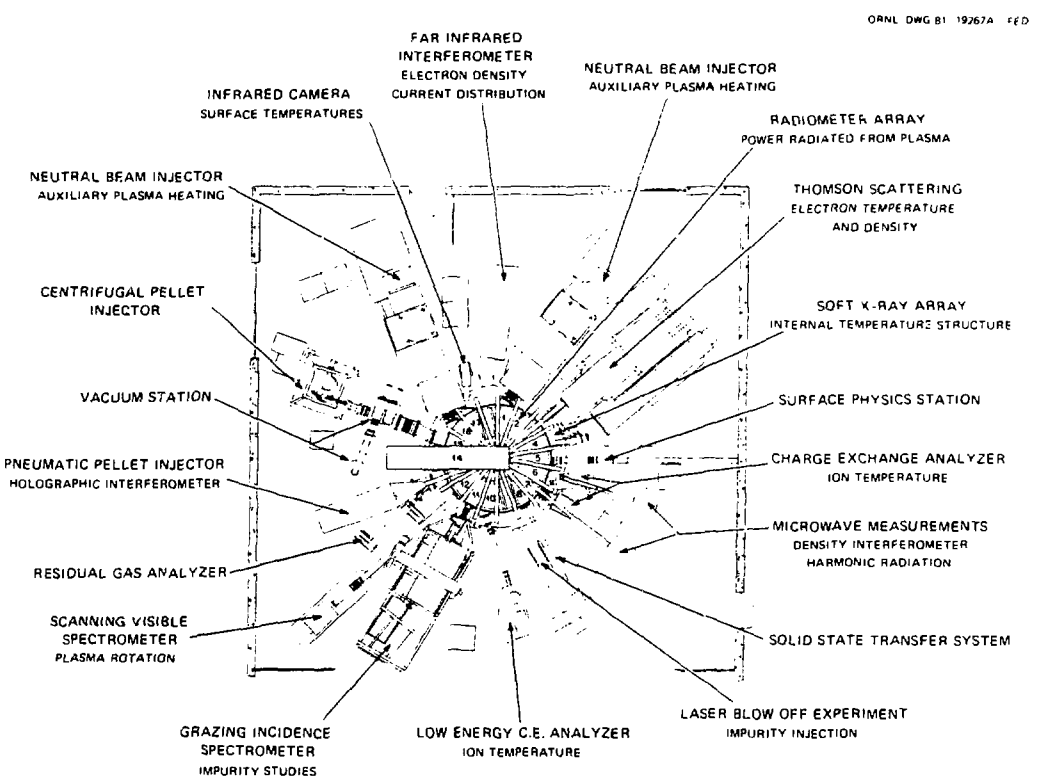

Fig. 2. Plan view of ISX-B with main diagnostic and auxiliary apparatus.

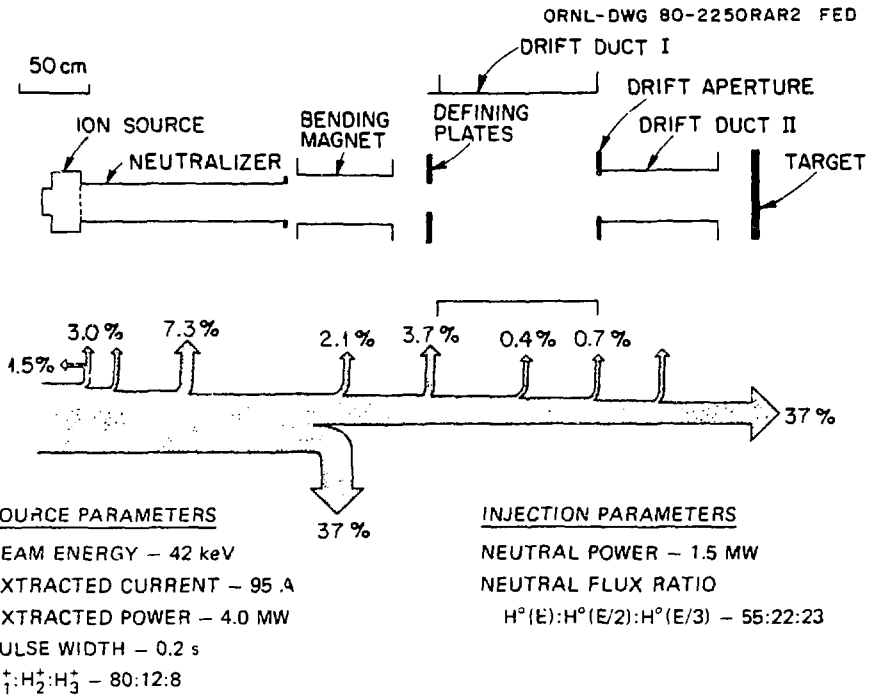

Fig. 3. Beam line schematic showing power flow and main operating parameters.

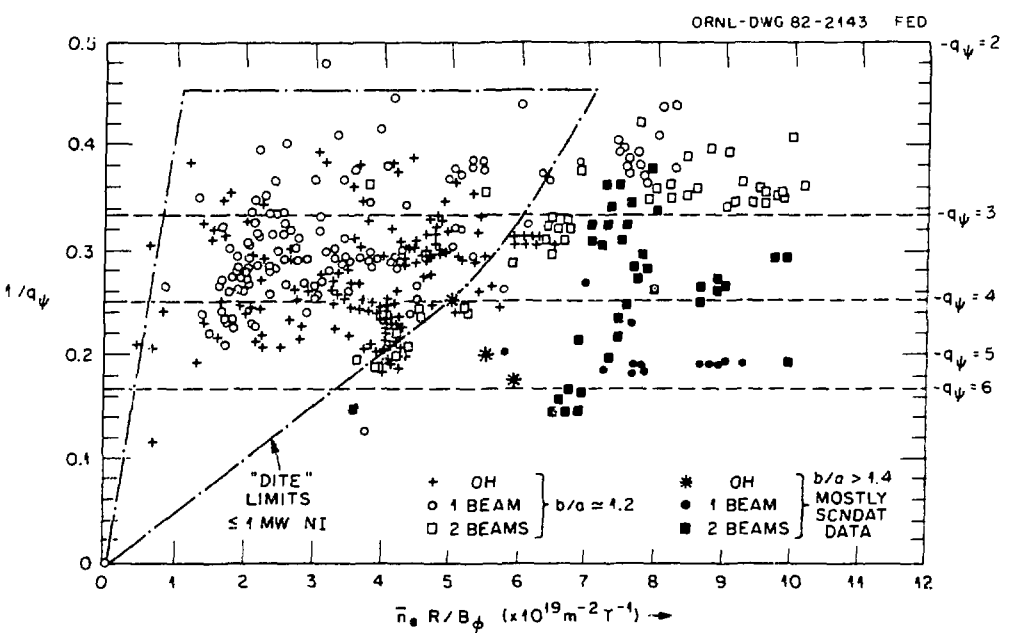

Fig. 4. Operating parameter range of the ISX-B experiment.

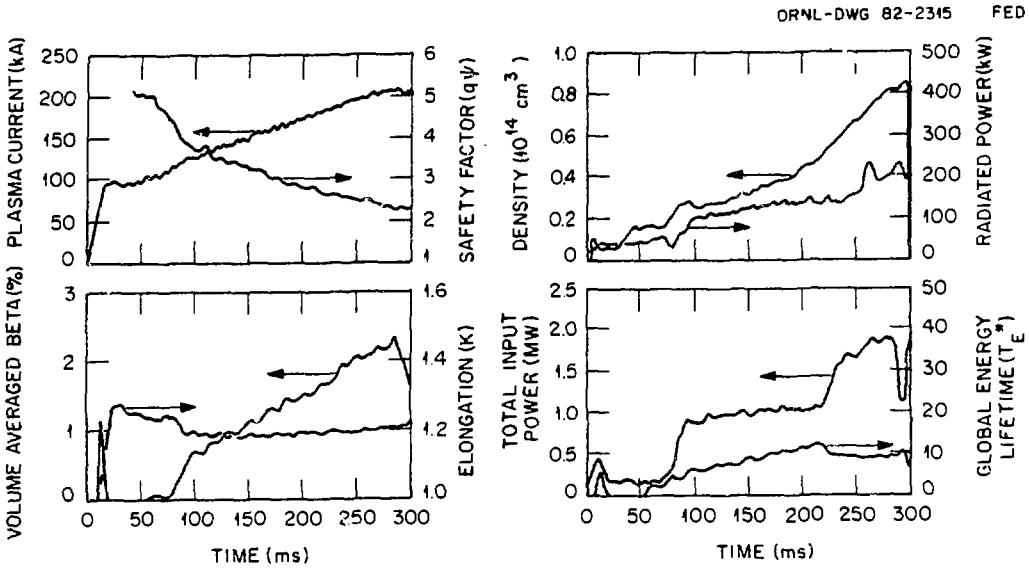

Fig 5. Characteristics of high beta ISX-B discharge as a function of discharge time: (a) I_p and q_a, (b) n_e and P_{rad}, (c) $\langle\beta\rangle$ and κ, (d) total input power and τ_E^*.

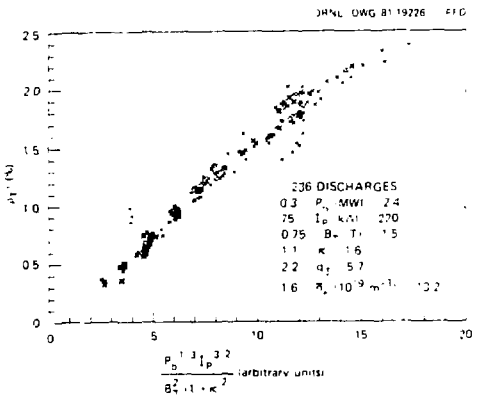

Fig. 6. Plot of $\langle\beta\rangle$ vs the empirical relationship, $I_p^{3/2}p_b^{1/3}/B_T^2(1+\kappa^2)$.

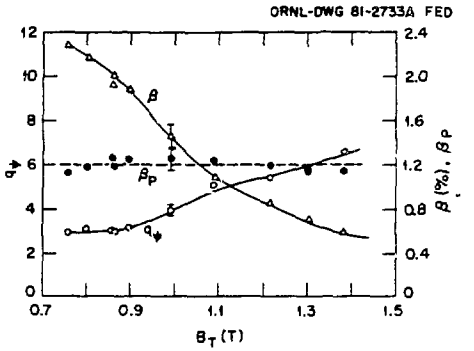

Fig. 7. Result of toroidal field scan.

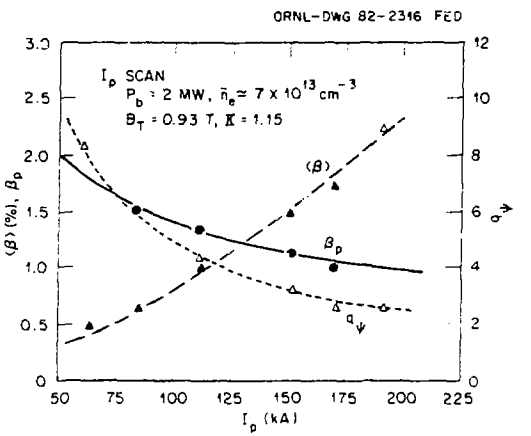

Fig. 8. Result of plasma current scan.

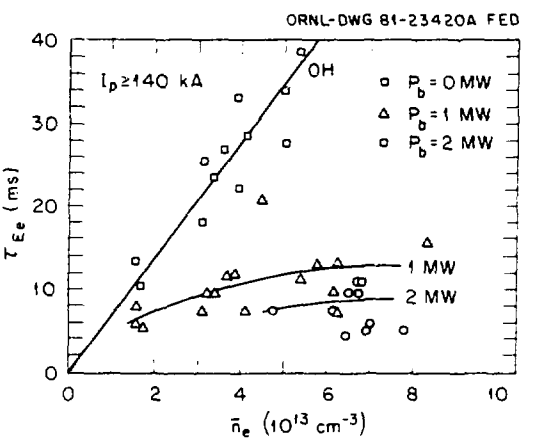

Fig. 9. Result of energy analysis calculation of electron confinement time vs density for various beam powers.

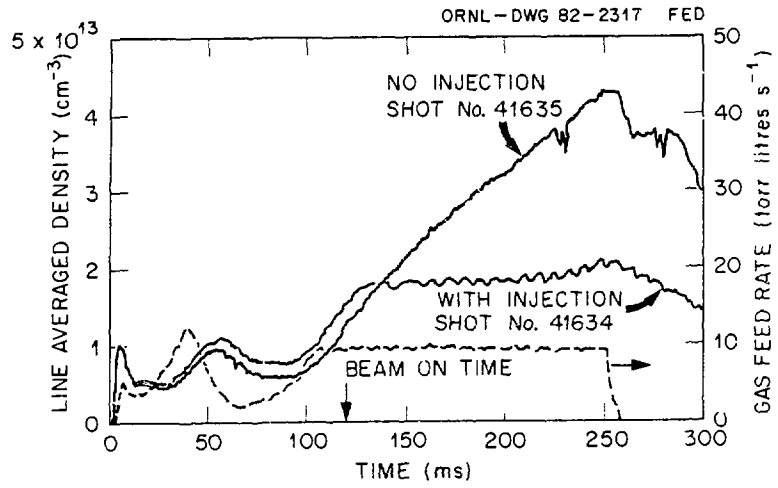

Fig. 10. Electron density history with and without neutral beam power for similar fueling rates (beam turn-on is at 120 ms).

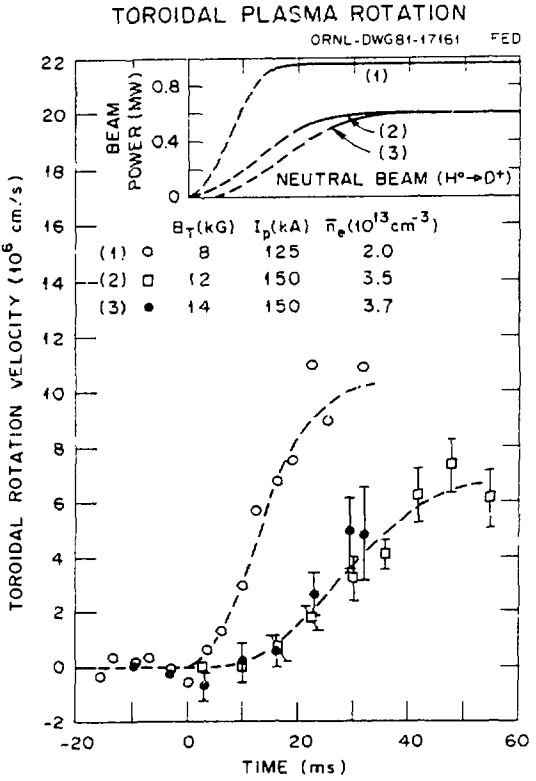

Fig. 11. Results of measurement of plasma rotation velocity from impurity Doppler shift measurements.

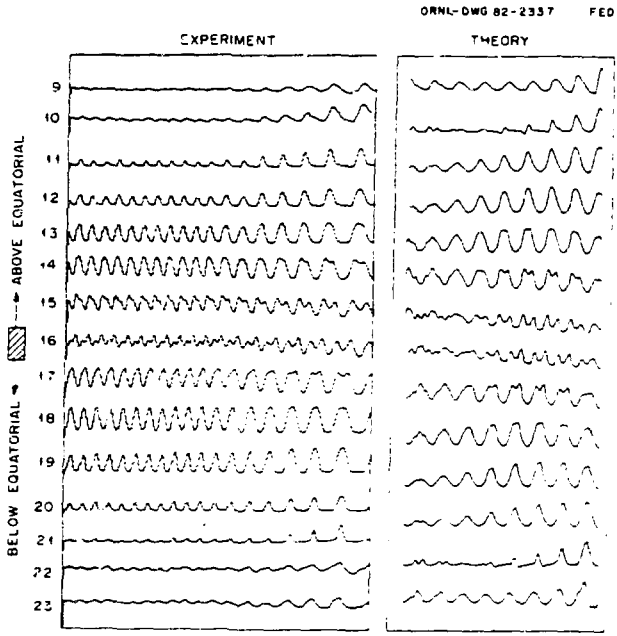

Fig. 12. Theoretically predicted and experimentally observed m/n = 1 MHD mode waveforms.

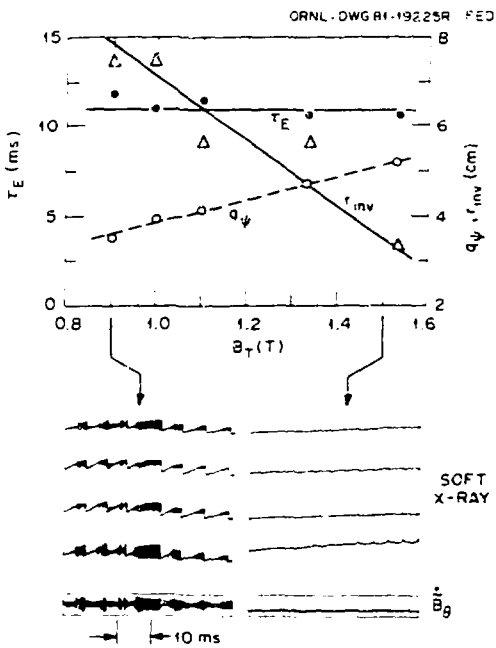

Fig. 13. Plot of B_T single parameter scan with associated MHD activity.